Revista Brasileira de Farmacognosia 28 (2018) 658–668

Brazilian Journal of Pharmacognosy
REVISTA BRASILEIRA DE FARMACOGNOSIA
www.elsevier.com/locate/bjp

Original Article

Application of high performance liquid chromatography and Fourier-transform infrared spectroscopy techniques for evaluating the stability of *Orthosiphon aristatus* ethanolic extract and its nano liposomes

Armaghan Shafaei, Mohammed Ali A. Saeed, Mohd Shahrul R. Hamil, Zhari Ismail*

Department of Pharmaceutical Chemistry, School of Pharmaceutical Sciences, Universiti Sains Malaysia, Minden, Penang, Malaysia

ARTICLE INFO

Article history:
Received 26 October 2017
Accepted 2 July 2018
Available online 13 September 2018

Keywords:
Stability
Nano liposomes
HPLC
FTIR
PCA

ABSTRACT

Orthosiphon aristatus (Blume) Miq., Lamiaceae, is a medicinal plant from Southeast Asia. Pharmacological effects of *O. aristatus* are attributed to the presence of lipophilic flavones. This study aimed to carry out accelerated stability studies on *O. aristatus* ethanolic extract and its nano liposomes. The extracts were exposed to four different temperatures at 30, 40, 50 and 60 °C for 6 months. The samples were analyzed at 0, 1, 2, 3, 4, 5 and 6 months by high performance liquid chromatography using rosmarinic acid, 3′-hydroxy-5,6,7,4′-tetramethoxyflavone, sinensetin and eupatorin as markers. Different chemical kinetic parameters of the markers were evaluated by Arrhenius equation to predict shelf life (t_{90}) at different storage conditions and at room temperature. Moreover, the stability of *O. aristatus* ethanolic extract and *O. aristatus* nano liposomes were analyzes by chemical fingerprinting using FTIR spectroscopy, principal component analysis and hierarchical clustering analysis. The degradation of markers in both *O. aristatus* ethanolic extract and *O. aristatus* nano liposomes followed the first order degradation reaction (dependening on their initial concentration). The loss of marker compounds in *O. aristatus* ethanolic extract, stored at 30, 40, 50 and 60 °C for six months were up to 25, 52, 72 and 89% for all compounds, respectively. However, in *O. aristatus* nano liposomes 16, 71, 85 and 100% of compounds were lost during 6 months of storage at 30, 40, 50 and 60 °C, respectively. Therefore, the markers in *O. aristatus* nano liposomes seems to be more stable at a temperature below 30 °C compared to *O. aristatus* ethanolic extract. However, markers present in *O. aristatus* ethanolic extract are more stable at a higher temperature (above 30 °C). principal component analysis or hierarchical clustering analysis analyses were applied to the FTIR results in order to demonstrate the discrimination between extracts based on the storage conditions. The results show that the functional group of the components in the extracts and their chemistry relationship is influenced by the temperature setup indicating the extracts are not stable during the storage conditions.

Introduction

Orthosiphon aristatus (Blume) Miq., Lamiaceae, is a medicinal plant grown in Southeast Asia, currently cultivated in Indonesia and Malaysia. In Malaysia, the leaves of this plant (misai kucing) have been used traditionally in treating angiogenesis related diseases, urinary lithiasis, oedema, inflammation, eruptive fever, influenza, hepatitis, jaundice, rheumatism, diabetes and hypertension (Akowuah et al., 2004). Various chemical constituents including flavonoids, terpenoids, saponins, hexoses, organic acids, chromene, myo-inositol and polyphenols have been identified in *O. aristatus* leaves extracts (Tezuka et al., 2000; Awale et al., 2001; Hossain and Mizanur Rahman, 2015). Numerous studies reported that lipophilic flavones such as 3′-hydroxy-5,6,7,4′-tetramethoxyflavone (TMF, 2), sinensetin (SIN, 3) and eupatorin (EUP, 4) and caffeic acid derivatives such as rosmarinic acid (RA, 1) present in leaves of *O. aristatus* possess potential therapeutic properties such as cytotoxic, anti-inflammatory and diuretic effects in rats (Dat et al., 1992; Akowuah et al., 2004; Yam et al., 2008; Sahib et al., 2009). Therefore, these compounds have been selected as markers of pharmacological activity by several researches (Akowuah et al., 2004; Yam et al., 2008; Sahib et al., 2009).

* Corresponding author.
E-mail: zhari@usm.my (Z. Ismail).

https://doi.org/10.1016/j.bjp.2018.07.005

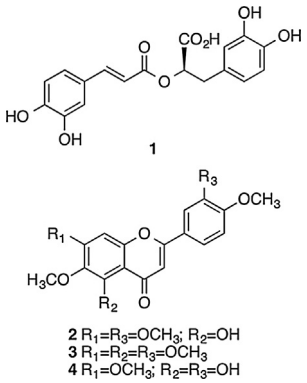

However, lipophilic flavones suffer from poor aqueous solubility which may limit their oral bioavailability. Therefore, OS ethanolic extract (OS-E) has been prepared in nano formulation form using liposomes from soybean phospholipids (OS-EL) (Abdalrahim et al., 2014). The liposomal formulation is usually used for increasing product stability, reduce toxicity, and improve bioavailability and efficacy compliance (Goyal et al., 2005; Fang and Bhandari, 2010; Munin and Edwards-Lévy, 2011).

The stability testing is important to ensure the standard dose-delivery of a drug throughout its shelf life and to fulfil legal requirements concerning identity, purity, strength and quality of a drug (Khalid et al., 2011). Furthermore, stability testing on pharmaceutical products permits the establishment of recommended storage conditions and shelf life. Hence, stability study of herbal products is very important in order to make reliable herbal remedies and medicines.

Due to insufficient analytical methods and difficulties in the quantification of constituents in herbal products the literature regarding the stability of herbal products is little. Purity and potency of herbal products were based on an un-scientific way, which was that the products retained as long as the appearance of a product remains unchanged. Therefore, it is necessary to carry out proper stability studies on plant extracts as well as other herbal products.

A number of methods have been used for stability assessment of herbal products such as metabolomics fingerprint profiling and quantification of marker compounds (Li et al., 2008; Hussain et al., 2009). The identification and phytochemical fingerprint using chromatographic and spectroscopic techniques may provide valuable information about qualitative and quantitative analysis of chemical composition in the medicinal herb in which pattern recognition can be achieved by using chemometric tools including principal component analysis (PCA) and hierarchical cluster analysis (HCA) (Zavoi et al., 2011).

Therefore, the aim of this study is to perform accelerated stability studies on ethanolic extract of OS and its nano liposomes. This study was carried out by using two techniques. The first was high performance liquid chromatography (HPLC) with four markers, RA (1), TMF (2), SIN (3) and EUP (4) as analytical markers for accelerated stability and chemical kinetics. The second approach was using Fourier-transform infrared (FTIR) for metabolite fingerprinting. Chemometric techniques, namely PCA and HCA were employed for the analysis of FTIR data. The findings from discrimination analyses of fingerprints using OS-E and OS-EL extracts keeping in different storage conditions are beneficial in identifying the differences or similarities of metabolite fingerprinting of the same extracts in various conditions.

Materials and methods

Chemicals and reagents

The pure standards ≥98% of RA (lot number: 1403450), TMF (lot number: 0305100), SIN (lot number: 09071507) and EUP (lot number: 1307358) were purchased from Indofine (New Jersey, USA). The solvent consisting of HPLC grade methanol and phosphoric acid were from Merck (Petaling Jaya, Selangor, Malaysia). Deionized water for HPLC was prepared using Ultra-pure water purifier system (Elgastat, Bucks, UK).

Plant materials

The *Orthosiphon aristatus* (Blume) Miq., Lamiaceae, leaves were purchased from a specialized supplier of herbal products in Malaysia (Herbagus Trading, Kepala Batas, Pulau Pinang) and identified at the herbarium of School of Biological Sciences Universiti Sains Malaysia, where a voucher sample was deposited (reference number: 11009).

Plant extraction

In preparing the extract, 100 g plant powder was added to 500 ml ethanol and mixed continuously on a magnetic stirrer for 48 h at 50 °C. After cooling, extracts were filtered using Whatman filter paper No. 1 (Whatman, England), concentrated at 50 °C under vacuum using a rotary evaporator (RE121 Buchi, Switzerland), and dried using a freeze-drying system (Labconco, USA).

Preparation of liposomes of Orthosiphon aristatus *ethanolic extract (OS-EL) in deoiled soya lecithin*

Orthosiphon aristatus ethanolic extract was prepared by the film method according to the method described by Abdalrahim et al. (2014). Briefly, purified soybean phospholipids from food grade soybean lecithin were dissolved in chloroform and OS-E extract was dissolved in methanol, the solutions were mixed, and the solvent was evaporated under vacuum using rotary evaporator at 45 °C for 30 min, followed by drying in an oven at 60 °C for 1 h. The OS-EL were characterized by solubility, entrapment efficiency, Fourier transform infrared spectroscopy (FTIR), transmission electron microscopy (TEM) and particle size and zeta potential (Abdalrahim et al., 2014).

High performance liquid chromatography (HPLC)

Instrumentation

The HPLC was performed using an Agilent Technologies series 1260 infinity (Waldronn, Germany) system equipped with a quaternary pump (G 1311 C), auto sampler (G 1329 B), column oven (G 1316 A) and ultraviolet (UV) detector (G 1314 F).

Preparation of standard compounds and samples

For the preparation of standard compounds stock solution, 5 mg of each standard was dissolved in 5 ml of methanol and then filtered through a 0.45 μm filter (Whatman). A series of working standard solutions were prepared by diluting the above solution with methanol. OS-E and OS-EL (100 mg) were dissolved in 10 ml of HPLC grade methanol. Working sample solutions of a concentration of 5 mg/ml were prepared by diluting the stock solutions with HPLC grade methanol. The samples were filtered through a 0.45 μm filter (Whatman).

Chromatographic conditions

The HPLC analysis was performed according to previously published method (Siddiqui and Ismail, 2011). The Nucleosil C18 column (250 × 4.6 mm internal diameter × 5 μm particles size) (Macherey Nagel, Germany) was used for analysis of RA (1), TMF (2), SIN (3) and EUP (4). The column temperature was maintained at

25 °C and the samples were injected at a volume of 20 μl. The compounds were eluted with an isocratic mobile phase comprising of methanol: tetrahydrofuran: water (0.1% H_3PO_4) mixture in the volume ratio 55:5:40. The flow rate was 0.7 ml/min and detection was carried out at 330 nm.

Validation of HPLC method

The developed HPLC method was validated in terms of linearity range, accuracy, precision, limit of detection (LOD), and limit of quantification (LOQ) according to the ICH guideline (ICH, 1996). The linearity of the method was determined as the regression coefficient (R^2) of calibration curve constructed at seven concentrations (0.5–1000 μg/ml). LOD and LOQ were measured based on the standard deviation of the response, and the slope was assessed according to the following equations:

$$\mathrm{LOD} = \frac{3.3\sigma}{S} \quad (1)$$

$$\mathrm{LOQ} = \frac{10\sigma}{S} \quad (2)$$

where σ is the standard deviation of the response and S is the slope of the calibration curve.

The RA, TMF, SIN and EUP content in OS-E and OS-EL extracts was calculated using calibration equation of reference compounds. The accuracy of the HPLC method was evaluated through recovery studies by adding known amounts of marker compounds solution (5, 250 and 500 μg/ml) into OS-E and OS-EL extracts. The spiked solutions were injected three times and the recovery was calculated using the value of detected, versus added amounts. The intra-day and inter-day precisions were determined for evaluation of method precision. The intra-day precision was evaluated by injecting three different concentrations of the standards (10, 250 and 500 μg/ml), six times for one day to HPLC system. The inter-day precision was obtained by injecting three different concentrations (10, 250 and 500 μg/ml) of the standards one time for six consecutive days. The resulting peak area was used to calculate standard deviation (SD) and the relative standard deviation (%RSD).

Instrumentation and FTIR measurements

FTIR spectra were obtained using Thermo Nicolet Nexus Infrared spectroscope coupled with an air-cooled Deuterated Triglycine Sulphate (DTGS) detector at resolution 4 cm^{-1} with sixteen interferograms co-added before Fourier transformation. The interferometer and detector chamber was purged with dry nitrogen to remove spectral interference due to atmospheric carbon dioxide and water vapour. The background spectrum spectra were recorded before analysis of the samples. Attenuated total reflectance (ATR) scan technique was used directly for all samples. The data were recorded at a mid-IR range of 400–4000 cm^{-1}.

Data processing for chemometric analysis

For FTIR data, the spectrum's baselines were corrected using Omnic software (Thermo Scientific, USA) to minimize the differences between spectra due to baseline shifts. The most intense band of peak absorbance was normalized and the spectra were then exported as Spectrum. SP file was imported into the multivariate statistical software programme. In this study, natural clustering of FTIR data was analyzed by PCA using The Unscrambler X (CAMO, Trondheim, Norway). Hierarchical clustering analysis (HCA) classification was employed on PCA data to discriminate the metabolites of each extract. The square Euclidean distance was employed to establish clusters in HCA and calculate dissimilarity coefficients, respectively.

Stability study protocol

The study was performed according to the protocol of the International Conference on Harmonization (ICH) as suggested by Working Party of Herbal Medicinal Products (WPHMP) of the European Agency for the Evaluation of Medicinal Products (EMEA, 2001; ICH, 2003). The OS-E and OS-EL samples, kept in screw caped transparent glass bottles, were exposed to four different storage conditions of temperatures in heating chamber (Binder, Fisher Scientific, USA) and relative humidity such as 30 °C/75% RH, 40 °C/75% RH, 50 °C/75% RH and 60 °C/75% RH for 6 months. The humidity was controlled by saturated aqueous salt solution (ASTM, 1991; Greenspan, 1977; Marsh, 1987; Young, 1967). The samples taken at 0, 1, 2, 3, 4, 5 and 6 months were analyzed in triplicate by HPLC and six replicate by FTIR. The storage duration was labelled as M0, M1, M2, M3, M4, M5 and M6.

Calculations of chemical kinetic parameters

Order of the reaction

The order of the reaction was determined using the graphic method (Murphy et al., 1997). Zero, first and second orders graphs were plotted from % remaining concentration versus time, the natural logarithm of % remaining concentration versus time and the inverse of remaining concentration ($1/C$) versus time, respectively for each temperature and the correlation coefficient of each graph was calculated. The plot with the best linearity was taken as the order of the chemical reaction. The reaction rate constant (K) for each marker compounds at different temperature was calculated from the slope of the curve.

Activation energy

Activation energy (Ea) is the energy required to move a molecule from initial state to the transitional state (which is frequently constant). The activation energy was calculated using Arrhenius equation. Degradation rate constant (K) was determined from the slope of the selected plot of the order of degradation reaction. The natural logarithm of the rate constant was plotted against the temperature ($1/T$) in Kelvin (Arrhenius equation) and the activation energy (Ea) was derived from the slope of the straight line of the plot ($-\mathrm{Ea}/2.303R$ or $-\mathrm{Ea}/R$).

The fraction of molecules having sufficient energy to move to the transitional state at a given temperature (A), was determined from the rate constant (K) by plotting logarithm ($\log K$) or natural logarithm ($\ln K$) versus reciprocal of the absolute temperature ($1/T$) (Pugh, 2002). The slope of the straight line of the plot ($-\mathrm{Ea}/2.303R$ or $-\mathrm{Ea}/R$) and intercept ($\log A$ or $\ln A$) were used to calculate Ea and A, respectively. The Arrhenius relationship was then used to determine the reaction rate constant at room temperature (25 °C, 298.15 K).

The Arrhenius equation is given as follows:

$$K = A\,e^{EQ/RT}$$

$$\mathrm{Ln}\,K = \mathrm{Ln}\,A - \frac{\mathrm{Ea}}{RT} \quad (3)$$

$$\mathrm{Log}\,K = \mathrm{Log}\,A - \frac{\mathrm{Ea}}{RT}$$

where K is a rate constant, A is frequency or collision factor, e is the base of natural logarithm, Ea is activation energy (J mol^{-1}), R is the universal gas constant (8.314 J $mole^{-1}$ k^{-1}) and T is temperature (K).

Shelf life (t_{90})

Shelf life depends on the order of the reaction and it is calculated using Arrhenius equation. The rate constant at different temperatures was used to estimate shelf life at various temperatures using the following equation for first order reaction.

$$\text{Shelf life } (t_{90}) = \frac{0.105}{K} \quad (4)$$

Results and discussion

Preparation of liposomes of Orthosiphon aristatus *ethanolic extract (OS-EL)*

The data obtained from characterization OS-EL were in line with a previous finding (Abdalrahim et al., 2014) (data are not shown). The results showed substantial enhancement of extract's solubility and entrapment efficiency. FTIR study indicates an interaction between soybean phospholipids and OS-E extract. TEM and dynamic light scattering showed the presence of round anionic nano liposomes with particle size and zeta potential of 152.5 ± 1.5 nm and −49.8 ± 1.1 mV, respectively.

Validation of HPLC method

Under the aforementioned HPLC conditions, complete base line separation of RA, TMF, SIN and EUP was achieved on a Nucleosil C_{18} column. RA (1), TMF (2), SIN (3) and EUP (4) were eluted at 6.2, 13.1, 16.8 and 20.6 min, respectively. The representative chromatograms of standard markers are shown in Fig. 1A. For both OS-E and OS-EL, the elution profile of reference markers is similar to that observed in their corresponding standards (Fig. 1). Linearity was evaluated by determining a series of seven concentrations of the standard solutions (0.5–1000 μg/ml) in three replicates. The linear regression equations and correlation coefficients were established from the graph by plotting the mean of peak area versus concentration. The standard solutions of the reference markers show a good linearity over the evaluated concentration range with $R^2 > 0.999$. The sensitivity of the method was evaluated by limit of detection (LOD) and limit of quantification (LOQ) analyses. The values of LOD and LOQ for all marker compounds were 0.02 and 0.2 μg/ml, respectively. The peak areas were used to calculate relative standard deviation (%RSD) of the reference compounds, and intra-day and inter-day precision rates. The variations were found to be in the range of 98.08–101.89% with RSD less than 3% for RA, 93.85–104.56% with RSD less than 1% for TMF, 97.12–107.49% with RSD less than 2% for SIN and 98.04–104.03% with RSD less than 3% for EUP. Percentage of

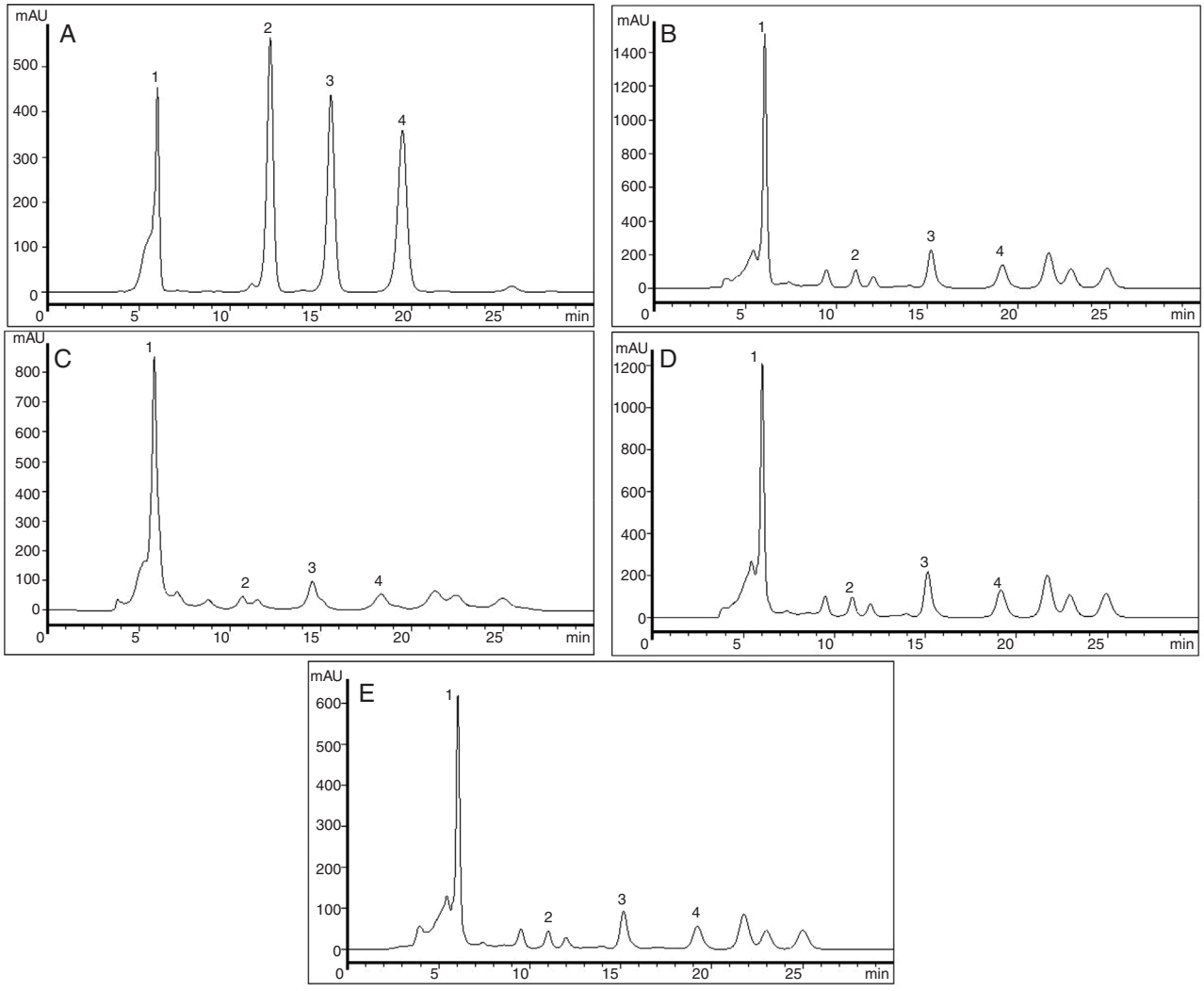

Fig. 1. HPLC chromatograms. (A) Marker compounds rosmarinic acid (**1**), 3′-hydroxy-5,6,7,4′-tetramethoxyflavone (**2**), sinensitin (**3**) and eupatorin (**4**), (B) ethanol extract of *Orthosiphon aristatus* (OS-E) stored at 30 °C/75% RH at month zero, (C) OS-E stored at 30 °C/75% RH at month six, (D) nano liposomes of ethanol extract of *O. aristatus* (OS-EL) stored at 30 °C/75% RH at month zero, and (E) OS-EL stored at 30 °C/75% RH at month six.

recovery for RA, TMF, SIN and EUP ranged between 97.26–103.80%, 98.20–103.60%, 98.27–102.37% and 99.17–100.74%, respectively with RSD less than 3%, indicating the applied method is reproducible.

The loss of marker compounds in OS-E stored at 30, 40, 50 and 60 °C/75% RH were found to be 24.88, 51.52, 56.8 and 89% for RA, 13.63, 17.76, 66.6 and 82.76% for TMF, 15.68, 23.53, 71.86 and 74.22 for SIN and 6.53, 17.08, 44.91 and 75.25% for EUP, respectively. Subsequently, decrease in marker compounds concentration in OS-EL stored at 30, 40, 50 and 60 °C/75% RH were 15.62, 70.19, 83.15 and 96.05% for RA, 11.33, 17.97, 81.77 and 100% for TMF, 11.16, 19.69, 84.37 and 95.13% for SIN and 15.24, 23.83, 75.51 and 100% for EUP, respectively. Results show that rising the temperature causes an increase in decomposition of marker compounds in the extracts which is in line with previous findings (Pourrat et al., 1995). It could be due to the lower integrity of the markers with extracts at a higher temperature. Our results are supported by findings of another study that found the rate of a chemical reaction increases by a factor between 2 and 3 times for each 10 °C rising in temperature (Pugh, 2002).

The orders of degradation reaction were calculated by plotting graphs of zero (time against remaining concentration), first (time against natural logarithm of remaining concentration (ln *C*)) and second order (time against the inverse of remaining concentration (1/*C*)) for each temperature. Regression correlation coefficient (R^2) of each graph was calculated and the graph with the best linearity was taken as an order of the reaction. By comparing different curves, it was found that markers followed the first order degradation reaction. Therefore, the rate of reaction is directly proportional to the concentration of one of the reactants and the rate constant (*K*) has a unit of sec^{-1} (S^{-1}).

The R^2 values for the first order graph of each temperature for RA, TMF, SIN and EUP in OS-E were in the range of 0.854–0.995, 0.806–0.962, 0.953–0.981 and 0.949–0.981, respectively. Subsequently, the values for RA, TMF, SIN and EUP in OS-EL were in the range of 0.958–0.987, 0.703–0.976, 0.714–0.985 and 0.867–0.950, respectively. These results indicate that degradation of the markers is dependent on their initial concentration. The reaction velocity or degradation rate constant (*K*) of the marker compounds at 30 °C, 40 °C, 50 °C and 60 °C were obtained from the slope of their curves for first order degradation reaction (time against natural logarithm of remaining concentration (ln *C*)). The rate constant of each marker compound at room temperature (25 °C) was determined from the data of linear regression by plotting the graph of (ln K) versus the inverse of temperature ($1/T$ $Kelvin^{-1}$). The Arrhenius plots of the reference markers are presented in Fig. 2. While degradation rate constant (*K*) of each reference marker at different temperatures is given in Table 1. The rate constants of degradation for all marker compounds were increased by about 2–3 fold as the storage temperature increased 10 °C which is in agreement with earlier findings (Rawlins, 1977). At high temperature (60 °C), the concentration of the marker compounds in OS-E and OS-EL had the greatest decrease which is attributed to the effect of the elevated temperature of storage that had caused an acceleration of the rate of degradation of the active substance.

Activation energy (Ea) was calculated from the slop of the straight line of a graph of ln K versus the inverse of temperature $1/T$ ($Kelvin^{-1}$) and universal gas constant ($R = 8.314$ kJ mol^{-1}). Whereas pre-exponential factor (*A*) was calculated from the intercept of the curve. The Ea and *A* of all the reference markers are presented in Table 1. The results illustrate that the activation energy of RA in both OS-E and OS-EL, is lower compared to TMF, SIN and EUP. Hence, the stability of RA is found to be less than other reference markers. Stability trend of reference markers for OS-E and OS-EL based on their activation energy is found in the order of EUP > TMF > SIN > RA. A similar trend is also found in values of the pre-exponential factor of the markers.

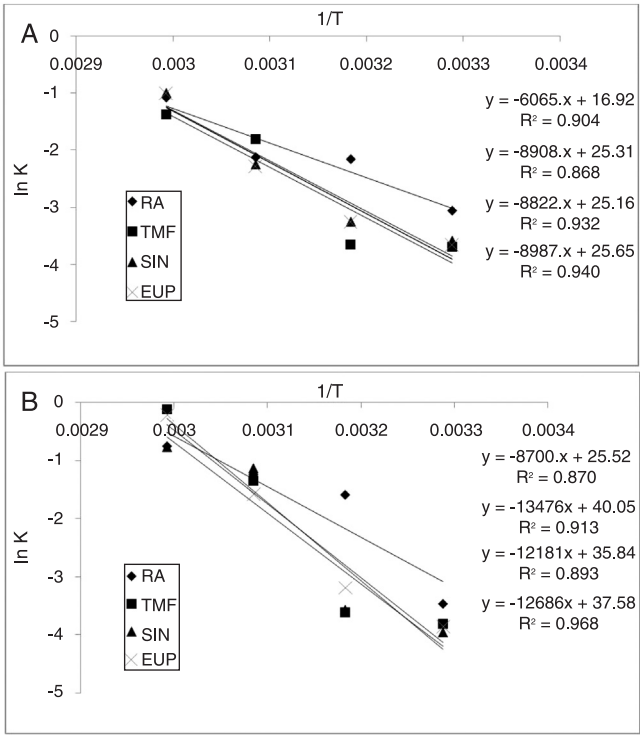

Fig. 2. Plot of natural log of rate constant versus inverse of temperature ($Kelvin^{-1}$) of RA, TMF, SIN and EUP in (A) *Orthosiphon aristatus* ethanolic extract (OS-E) and (B) nano liposomes of *O. aristatus* ethanolic extract (OS-EL) at various temperatures, ln *K* (natural log of rate constant); $1/T$ (inverse of temperature).

The markers followed the first order degradation reaction. Therefore, t_{90} of each reference marker was determined through dividing 0.105 by degradation rate constant (*K*). The estimated t_{90} of the markers at different storage conditions are given in Table 2. The results demonstrate that all marker compounds in OS-EL have a longer shelf life at 25 and 30 °C compared to OS-E. It might be due to a better combination of OS-E extract with liposomes drug delivery systems at a lower temperature. While, at higher temperature 40, 50 and 60 °C they have a shorter shelf life in OS-EL as compared to OS-E.

Stability study of OS-E and OS-EL by chemical fingerprinting using FTIR spectroscopy and principal component analysis

The results of Fourier transform infrared (FTIR) spectra analysis OS-E and OS-EL stored at 30 °C/75% RH and 60 °C/75% RH for six months are presented in Fig. 3. The results of principal component analysis (PCA) on the infrared spectra of OS-E and OS-EL stored at four different conditions for six months in the 400–4000 cm^{-1} spectral region are given in Figs. 4 and 5. Prior to the PCA analysis, the baseline of the FTIR spectra was corrected, smoothed and normalized. PCA analysis was carried out with PC-2 versus PC-1 analysis (PC-2 vs PC-1). In order to identify the peaks that contributed to the discrimination of extracts, loading plots of PC-1and PC-2 were also generated (Figs. 4 and 5).

PCA score plot for OS-E can explain more than 96% of the total variance (Fig. 4). In Fig. 4A, PCA plot contains four different groups. This plot illustrates the distribution of OS-E extracts stored at 30 °C/75% RH for six months. Group A consists of (M0 and M6), B (M1 and M2), C (M3 and M4) and D (M5). Groups A and B were clustered at negative PC-1 axis and groups C and D were clustered at the

Table 1
Rate constant (K), activation energy (Ea) and pre-exponential factor (A) of the RA, TMF, SIN and EUP of *Orthosiphon aristatus* ethanolic extract (OS-E) and its nano liposomes (OS-EL) stored at different temperatures.

Sample	Name of marker	K (S^{-1})25 °C	K (S^{-1})30 °C	K (S^{-1})40 °C	K (S^{-1})50 °C	K (S^{-1})60 °C	Ea (kJ mol^{-1})25 °C	A (S^{-1})
OS-E	RA	0.031	0.047	0.116	0.12	0.341	50.42	21492422.68
	TMF	0.013	0.025	0.026	0.164	0.254	74.06	131109766320.81
	SIN	0.015	0.028	0.039	0.106	0.37	73.34	110676147752.24
	EUP	0.014	0.026	0.039	0.102	0.367	74.71	176795881648.57
OS-EL	RA	0.019	0.031	0.202	0.286	0.466	72.33	90163989355.77
	TMF	0.010	0.022	0.027	0.258	0.883	112.03	444856496010320000
	SIN	0.009	0.019	0.028	0.319	0.46	101.27	5361992500000040
	EUP	0.010	0.021	0.041	0.205	0.801	105.47	31351467997242200

Table 2
Shelf life (t_{90}) of the markers in *Orthosiphon aristatus* ethanolic extract (OS-E) and its nano liposomes (OS-EL) at different storage conditions.

Sample	Name of Marker	t_{90} (months)25 °C	t_{90} (months)30 °C	t_{90} (months)40 °C	t_{90} (months)50 °C	t_{90} (months)60 °C
OS-E	RA	3.33	2.23	0.905	0.875	0.307
	TMF	7.57	4.2	4.03	0.640	0.413
	SIN	6.72	3.75	2.69	0.990	0.283
	EUP	7.319	4.03	2.69	1.029	0.286
OS-EL	RA	5.48	3.38	0.519	0.367	0.225
	TMF	10.05	4.77	3.88	0.406	0.118
	SIN	10.84	5.52	3.75	0.329	0.228
	EUP	10.08	5	2.56	0.512	0.131

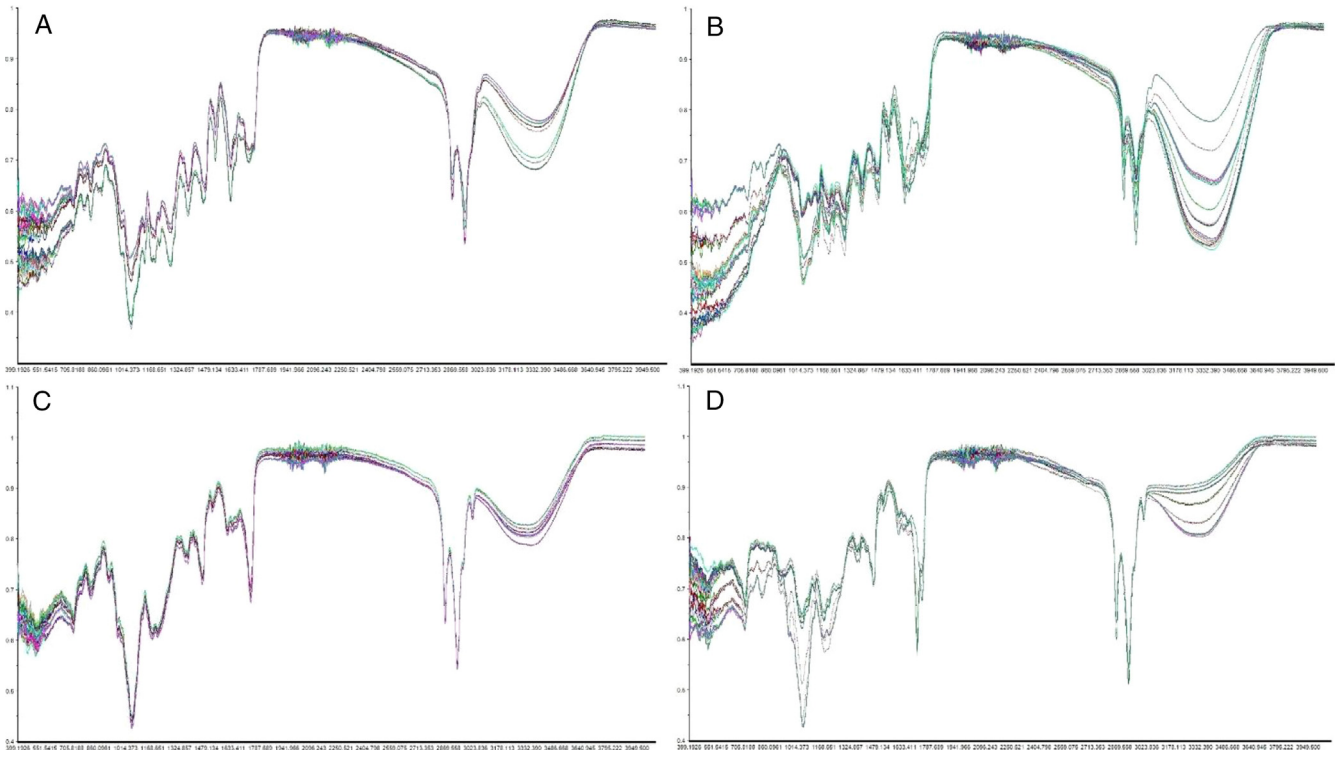

Fig. 3. Fourier transform infrared (FTIR) spectra of (A) ethanolic extract of *Orthosiphon aristatus* (OS-E) stored at 30 °C/75% RH; B. OS-E stored at 60 °C/75% RH; C. Nano liposomes of ethanol extract of *O. aristatus* (OS-EL) stored at 30 °C/75% RH, and D. OS-EL stored at 60 °C/75% RH for six months.

positive PC-1 axis. Those extracts stored at 40 °C/75% RH showed five groups consisting of A (M0), B (M1 and M2), C (M3), D (M4 and M6) and E (M5) (Fig. 4B). Groups A, C and D were clustered at negative PC-1 axis and groups B and E were clustered at the positive PC-1 axis. The results revealed that peak at 1000–1120 cm^{-1} (C–O–C stretching) and peak at 2850–2920 cm^{-1} (C–H stretching or vibration of saturated an unsaturated hydrocarbons) are the main variants for positive and negative PC-1 loading, respectively in Fig. 4A and B. While, peak at 1600–1760 cm^{-1} (amino acids, terpenoids and flavonoids) and peak at 1330–1420 cm^{-1} (O–H) contribute for clustering negative PC-2 in Fig. 4A and B, respectively. Positive loading of PC-2 in Fig. 4A and B are attributed to peak at 2850–2920 cm^{-1}.

The extracts stored at 50 °C/75% RH showed three groups of A (M0 and M2), B (M1, M3, M5 and M6) and C (M4). The position of these groups follows the clock directional path (Fig. 4C). Group A was clustered at the negative PC-1 axis and group B and C were clustered at the positive PC-1 axis. The peak at 1000–1120 cm^{-1} (C–O–C stretching) and 3000–3600 cm^{-1} (hydroxyl group) are the main variants for positive PC-1 loading, while, peak at 2850–2920 cm^{-1} (C–H stretching or vibration of saturated an unsaturated hydrocarbons) is the main variants for negative PC-1 loading. Furthermore,

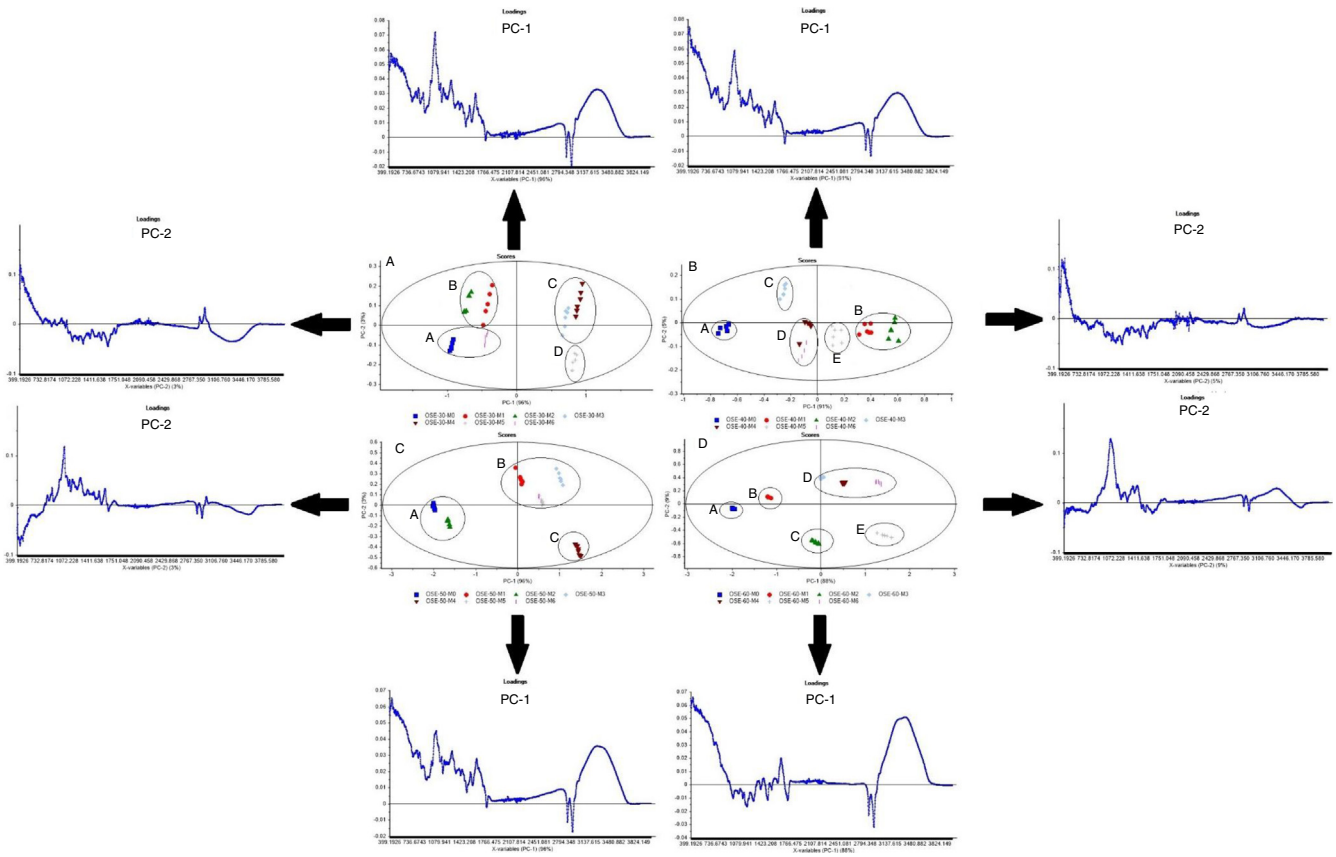

Fig. 4. PCA plots, PC-1 and PC-2 loading plots of ethanolic extract of *Orthosiphon aristatus* (OS-E) stored at (A) 30 °C/75% RH; (B) 40 °C/75% RH; (C) 50 °C/75% RH and (D) 60 °C/75% RH for six months.

negative and positive loading of PC-2 are contributed to peak at 900–1200 cm^{-1} (carbohydrates) and 1420–1330 cm^{-1} (O–H) (Fig. 4C).

The extracts stored at 60 °C/75% RH showed five groups including A (M0), B (M1), C (M2), D (M3, M4 and M6) and E (M5) (Fig. 4D). Groups A, B and C were clustered at negative PC-1 axis and groups D and E were clustered at the positive PC-1 axis. The peak at 3000–3600 cm^{-1} (hydroxyl group) and peak at 1000–1120 cm^{-1} (C-O-C stretching) are the main vibration for positive and negative PC-1 loadings, respectively. Moreover, peaks at 900–1200 cm^{-1} (carbohydrates) and 1600–1760 cm^{-1} (amino acids, terpenoids and flavonoids) are the main variants for positive and negative loadings of PC-2, respectively (Fig. 4D).

Fig. 5 depicts the PCA score plot of the OS-EL extracts which can explain more than 81% of the total variance. OS-EL extracts stored at 30 °C/75% RH containing four different groups. Group A consists of (M0 and M5), B (M1, M2 and M4), C (M3) and D (M6). Groups A and D are clustered at the positive PC-1 axis and group B and C are clustered at negative PC-1 axis (Fig. 5A). Those extracts stored at 40 °C/75% RH show 4 groups consisting of A (M0, M1 and M2), B (M3), C (M4 and M5) and D (M6) (Fig. 5B). Groups A and B are clustered at positive PC-1 axis and groups C and D in the negative PC-1 axis. From the PC-1 and PC-2 loading plots, it could be indicated that peaks at 3000–3600 cm^{-1} (hydroxyl group) and 1600–1760 cm^{-1} (amino acids, terpenoids and flavonoids) are the main variants for positive and negative PC-1 loadings, respectively in Figs. 5A and B. However, peaks at 3000–3600 cm^{-1} (hydroxyl group) and 1000–1120 cm^{-1} (C–O–C stretching) are the main variants for positive and negative PC-2 loadings, respectively in Fig. 5A. However, in Fig. 5B the main variant related to positive and negative loadings of PC-2 is related to peak at 1600–1760 cm^{-1} (amino acids, terpenoids and flavonoids).

The extracts stored at 50 °C/75% RH show three groups of A (M0, M1 and M6), B (M2, M3 and M4) and C (M5). The position of these groups follows the clock directional path (Fig. 5C). Group A and B are clustered at the negative PC-1 axis and group C is clustered at the positive PC-1 axis. The peaks at 1600–1760 cm^{-1} (amino acids, terpenoids and flavonoids) and 2850–2920 cm^{-1} (C–H stretching or vibration of saturated an unsaturated hydrocarbons) are the main variants for positive and negative PC-1 loadings, while, peaks at 900–1200 cm^{-1} (carbohydrates) and 1600–1760 cm^{-1} (amino acids, terpenoids and flavonoids) are the main variants for positive and negative PC-2 loadings, respectively (Fig. 5C).

The extracts stored at 60 °C/75% RH show three groups including A (M0), B (M1 and M2) and C (M3, M4, M5 and M6) (Fig. 5D). Groups A and B and are located in positive PC-1 axis and group C is in the negative PC-1 axis. Peak at 1000–1120 cm^{-1} (C–O–C stretching) and peak at 1600–1760 cm^{-1} (amino acids, terpenoids and flavonoids) are the main vibrations for positive and negative PC-1 loadings, and peaks at 1000–1120 cm^{-1} (C–O–C stretching) and 1600–1760 cm^{-1} (amino acids, terpenoids and flavonoids) are the main vibrations for positive and negative PC-2 loadings (Fig. 5D).

Hierarchical clustering analysis for FTIR fingerprinting

In order to see the similarities and dissimilarities between FTIR fingerprints of extracts stored at different temperatures, cluster analysis was conducted using UnscramblerX (CAMO, Trondheim, Norway). The Ward' hierarchical clustering method with Euclidean distance was used in this study. The HCA analysis on OS-E extracts stored at 30 °C/75% RH confirm the close grouping of A and B as well as the different individual clusters of C and D. Subsequently, the HCA results of OS-E stored at 40 °C/75% RH confirm the similarity of groups A, C and D and dissimilarity with groups B and E.

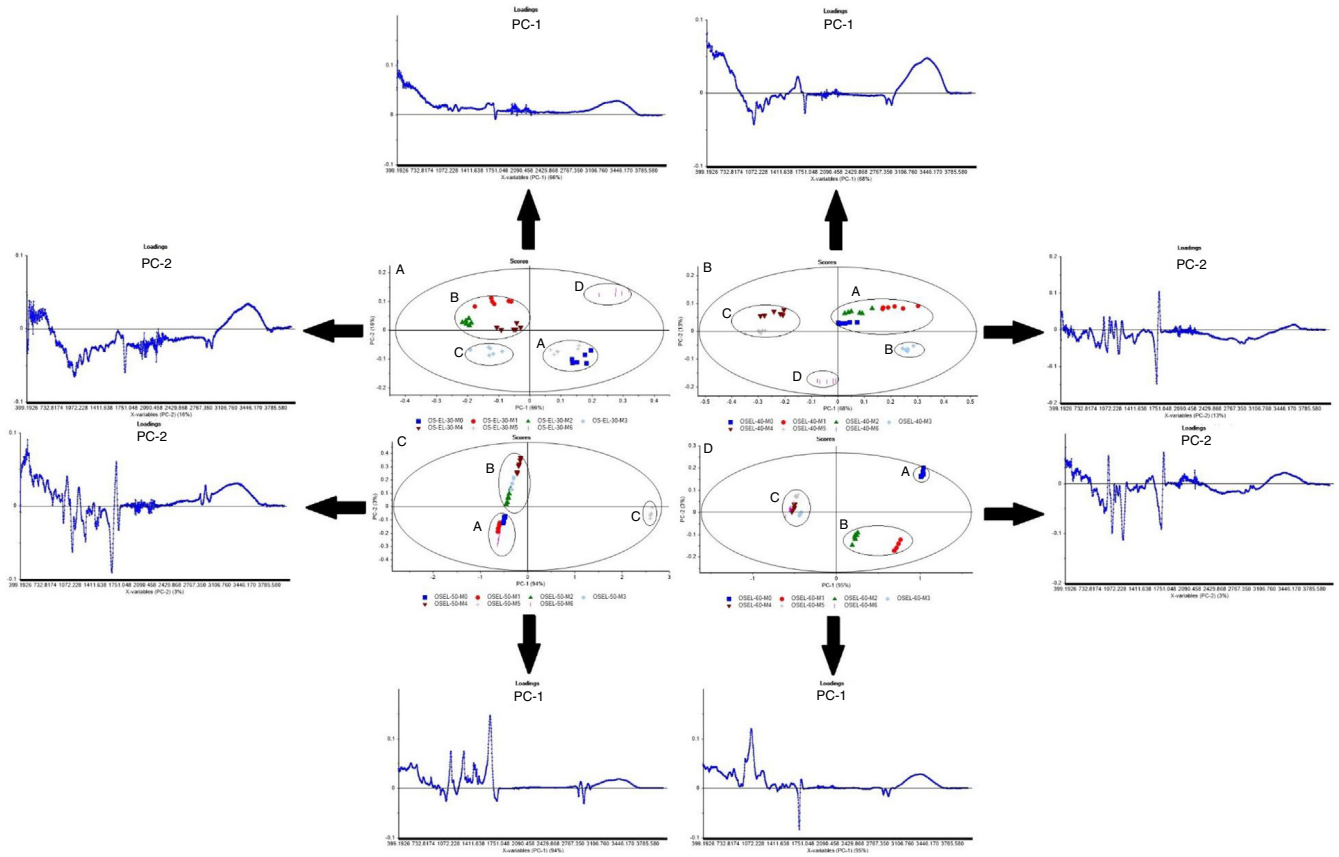

Fig. 5. PCA plots, PC-1 and PC-2 loading plots of nano liposomes of ethanolic extract of *Orthosiphon aristatus* (OS-EL) stored at (A) 30 °C/75% RH; (B) 40 °C/75% RH; (C) 50 °C/75% RH and (D) 60 °C/75% RH for six months.

Furthermore, HCA analysis of OS-E extracts stored at 50 °C/75% RH shows similarity of groups B and C and dissimilarity with group A. Finally, the HCA of OS-E extracts stored at 60 °C/75% RH proves similarity of groups A and B and dissimilarity with groups D and E (Fig. 6).

Hierarchical clustering analysis analysis in OS-EL extracts stored at 30 °C/75% RH shows a close grouping of A and D and their differences with B and C. In OS-EL extracts stored at 40 °C/75% RH similarity of groups A and B and dissimilarity with groups C and D are confirmed. HCA analysis in OS-EL extracts stored at 50 °C/75% RH and 60 °C/75% RH also are in good agreement with PCA pattern as discussed above. The samples with similar chemical profiles are clustered into the same subgroups. It has to be noted that HCA summarizes the whole spectral data in a plot showing the relationship between different samples. The FTIR spectral data from stability study of OS-E and OS-EL extracts stored at different conditions for 6 months shows that the PCA and HCA techniques are capable of differentiating the extracts according to their similarity in chemical profiling (Figs. 4–6).

Orthosiphon aristatus plant is rich in flavonoids and phenolic derivatives which has shown different pharmacological activities (Dat et al., 1992; Akowuah et al., 2004; Yam et al., 2008; Sahib et al., 2009). Therefore, stability study of flavonoids and phenolic derivatives in *O. aristatus* plant under different conditions is a very important aspect that must be taken into account to ensure that phenolic compounds possess the desired properties and maintain their activity under different storage conditions, which can involve high temperatures (Volf et al., 2014). Stability studies provide evidence on the influence of environmental factors on the time on the quality of a drug substance (WHO, 1996). Stability studies are the first assessment of chemical constancy of a drug before developing a dosage. Furthermore, stability testing is useful to predict the shelf life of medical products as well as their storage conditions. On the whole, the stability studies which involve examining the quality and potentiality of a product at suitable time intervals are conducted to calculate the kinetics of each marker compounds for determination degradation order. The degradation of marker compounds in this study was demonstrated to be a first-order kinetic reaction. In other words, the percentage remaining concentrations were decreased with the increase in storage temperature.

Stability of a marker compound in plant extracts is affected by numbers of physical factors such as temperature, moisture and light, and chemical factors such as hydrolysis, oxidation, polymerization and isomerization. The rates of degradation of active ingredients are increased by enhancing temperature due to an increase in their kinetic energy which results in increasing the fraction of colliding molecules. The products are susceptible to hydrolysis and decomposition in the present of moisture (Waterman et al., 2002). As known, the selected marker compounds in this study belong to flavonoid and phenolic classes. The hydroxyl groups present in the structure of flavonoid and phenolic compounds, make them accessible to hydrolysis and oxidation. Hydrolysis and oxidation are the main reasons behind the degradation of flavonoids and phenolic compounds (Kotsiou and Tasioula-Margari, 2016). According to (Bruneton, 1999; Friedman and Jürgens, 2000), the characteristic of flavonoids (solubility in water, sensitivity to the metal ion, ultraviolet radiation and the hydrolysis) were accelerated directly or proportionally by the increase in the temperature. Ameena et al. showed the immense effect of storage temperature on the stability of the phenolic

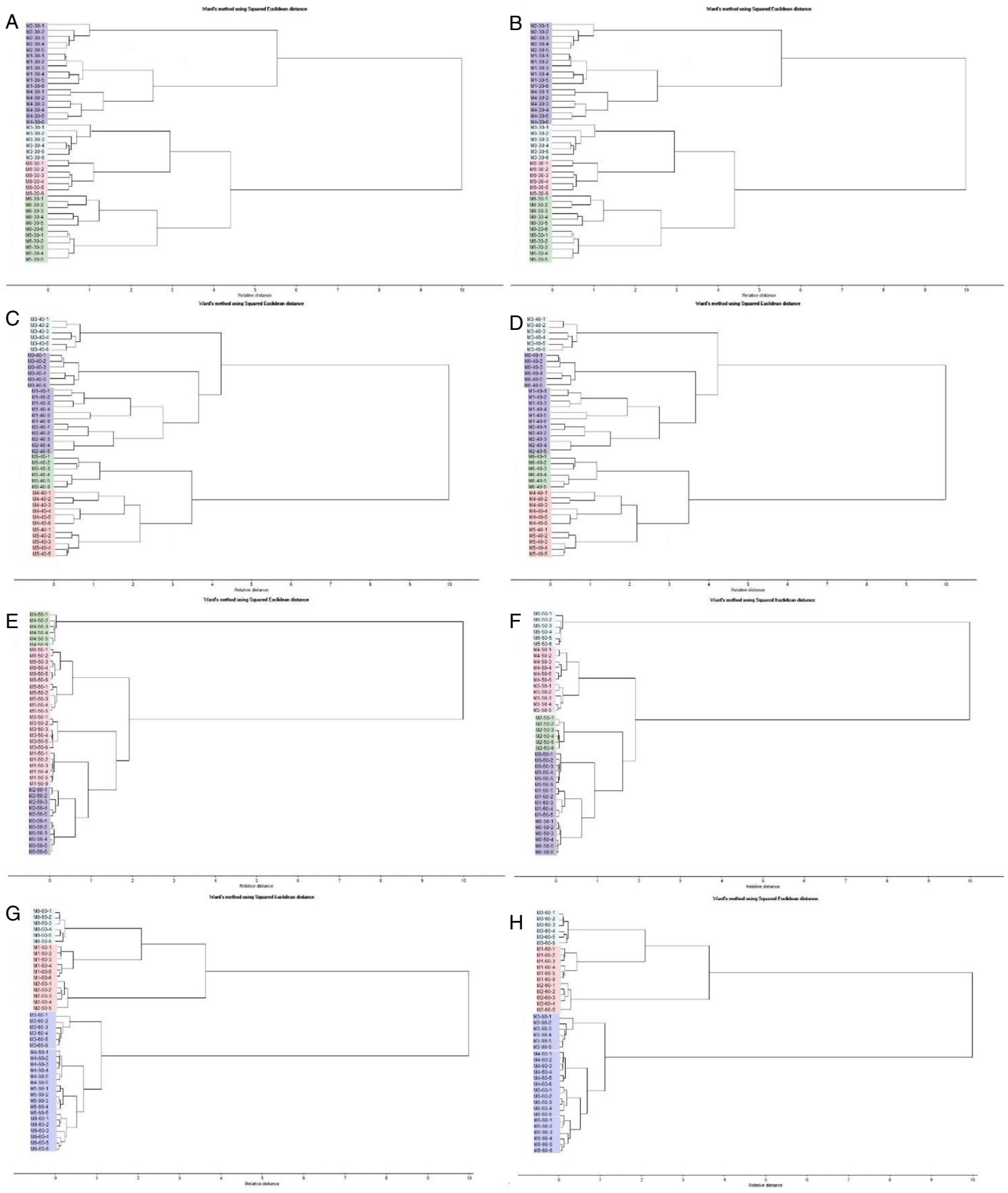

Fig. 6. HCA dendograms of (A) ethanolic extract of *Orthosiphon aristatus* (OS-E) stored at (A) 30 °C/75% RH; (B) nano liposomes of ethanolic extract of *O. aristatus* (OS-EL) stored at 30 °C/75% RH; (C) OS-E stored at 40 °C/75% RH; (D) OS-EL stored at 40 °C/75% RH; (E) OS-E stored at 50 °C/75% RH; (F) OS-EL stored at 50 °C/75% RH; (G) OS-E stored at 60 °C/75% RH; and (H) OS-EL stored at 60 °C/75% RH for six months.

compounds which can be facilitated in the presence of light (Ali et al., 2018). Corroborating with the present study, similar hydrolysis and oxidative reactions could have taken place in both OS-E and OS-EL especially at a higher temperature (above 30 °C) and lead to the subsequent decrease in the content of marker compounds.

Different phenolics behave in a different manner when it comes to their degradation and this diverse behaviour could be attributed to their structural differences. The reactivity of compound is dependent on the position of the functional groups. Positions 3 and 4 in the benzene ring of flavonoids are more susceptible to

dihydroxylation than others (Rice-Evans et al., 1996). Hydroxylation decreases the stability, whereas methylation increases the stability of a compound (Bąkowska-Barczak, 2005). As no detailed literature exists on the degradation mechanism of the flavonoid and phenolic compounds in *O. aristatus* extracts, it is possible that similar hydroxylation of the hydroxyl group in TMF and EUP took place leading to their degradation. Similarly, it can only be assumed that the different structural variation including the number and position of diverse functional groups present in RA and SIN could affect their reactivity and consequent degradation (Ali et al., 2018).

The assessment of the quality of OS-E and OS-EL extracts in this accelerated short-term stability studies were also analyzed qualitatively using FTIR. Absorption bands within FTIR spectra are associated with stretching or vibration of particular chemical bonds. Depending on the nature of the samples presented in the analysis, these absorption patterns can be used to characterize the differences in metabolites composition and track temporal changes in this composition (Elliott et al., 2007). As displayed, under similar conditions, the extracts that have similar functional group can be clustered together in the same position. However, under different storage conditions, same extracts are clustered in different positions. The results show that the functional group of the components in the extracts and their chemistry relationship has been influenced by the temperature setup indicating the extracts are not stable during the storage conditions.

From the results, it could be concluded that both OS-E and OS-EL extracts were more stable at 25 °C compared to the other studied temperatures. According to HPLC results a decrease in the remaining concentration of all marker compounds occurred over six months storage. However, the degradation of marker compounds was found to be faster in high temperature. The degradation of marker compounds for both OS-E and OS-EL extracts followed the first order degradation reaction. The overall quality of the OS-E and OS-EL extracts after six months was optimized at 25 °C. Shelf-life at the optimized storage condition from the first order kinetic model was determined as 3.33 and 5.48 months in OS-E and OS-EL, respectively. It is suggested that both OS-E and OS-EL should be stored at the optimum conditions as proposed in this study. However, storage in refrigeration condition could increase the shelf life of flavonoid and phenolic compounds (Del-Toro-Sánchez et al., 2015). Therefore, further investigation of the effect of refrigeration condition on the stability of flavonoid and phenolic compounds available in OS extracts is necessary to be done. In addition, investigation of the effect of physicochemical parameters such as monitoring the particle size and zeta potential on nano liposomes of OS-E extract (OS-EL) stability stored at different temperatures over six months storage is needed to be done in future.

The FTIR study shows the discrimination between extracts based on storage conditions. The results demonstrate that identification of the most similar samples based on their metabolites profile as well as the most different ones can be easily established using either chemometric analyses of PCA or HCA. To the best of our knowledge, studies on the stability of the extract based on metabolites profiling using chromatographic and spectroscopic techniques combined with chemometrics tools are scanty. So, this is the first report presenting such an elaborate study. Findings from this study can be employed as a template for the quality of plant extract for further product development study.

Authors' contributions

ZI designed the study and assisted AS (PhD student), MAAS (PhD student) and MSRH (MSc student) in conducting the study. AS, MAAS and MSRH interpreted the data, and AS and ZI drafted the manuscript. All authors reviewed the data and approved the final version of the manuscript.

Conflicts of interest

The authors declare no conflicts of interest.

Acknowledgment

The authors would like to acknowledge Universiti Sains Malaysia for the financial support given under the USM Fellowship Scheme. This project was funded by the Malaysian Ministry of Agriculture and Agro-Based Industry, NKEA Research Grant Scheme (NRGS), Ref. No.: 304/PFRMASI/650738/K123.

Appendix A. Supplementary data

Supplementary data associated with this article can be found, in the online version, at doi:10.1016/j.bjp.2018.07.005.

References

Abdalrahim, F.A.A., Amin Malik, S.A.M., Zhari, I., 2014. Preparation and characterization of nano liposomes of *Orthosiphon stamineus* ethanolic extract in soybean phospholipids. BMC Biotechnol. 14, http://dx.doi.org/10.1186/1472-6750-14-23.

Akowuah, G.A., Zhari, I., Norhayati, I., Sadikun, A., Khamsah, S.M., 2004. Sinensetin, eupatorin, 3′-hydroxy-5,6, 7,4′-tetramethoxyflavone and rosmarinic acid contents and antioxidative effect of *Orthosiphon stamineus* from Malaysia. Food Chem. 87, 559–566.

Ali, A., Chong, C., Mah, S., Abdullah, L., Choong, T., Chua, B., 2018. Impact of storage conditions on the stability of predominant phenolic constituents and antioxidant activity of dried *Piper betle* extracts. Molecules 23, http://dx.doi.org/10.3390/molecules23020484.

ASTM, 1991. Standard practice for maintaining constant relative humidity by means of aqueous solution. In: Annual Book of ASTM Standards: Designation. American Society for Testing and Materials, Philadelphia, pp. 104–185.

Awale, S., Tezuka, Y., Banskota, A.H., Kouda, K., Tun, K.M., Kadota, S., 2001. Five novel highly oxygenated diterpenes of orthosiphon s tamineus from Myanmar. J. Nat. Prod. 64, 592–596.

Bąkowska-Barczak, A., 2005. Acylated anthocyanins as stable, natural food colorants – a review. Pol. J. Food Nutr. Sci. 14, 107–116.

Bruneton, J., 1999. Pharmacognosy, Phytochemistry and Medicinal Plants, 2nd ed. Lavoisier Publishing; Secaucus, Intercept, Paris.

Dat, D.D., Ham, N.N., Khac, D.H., Lam, N.T., Son, P.T., Dau, N.v., Grabe, M., Johansson, R., Lindgren, G., Stjernström, N.E., 1992. Studies on the individual and combined diuretic effects of four Vietnamese traditional herbal remedies (*Zea mays*, *Imperata cylindrica*, *Plantago major* and *Orthosiphon stamineus*). J. Ethnopharmacol. 36, 225–231.

Del-Toro-Sánchez, C.L., Gutiérrez-Lomelí, M., Lugo-Cervantes, E., Zurita, F., Robles-Garc, M.A., Ruiz-Cruz, S., Aguilar, J.A., Morales-Del Rio, J.A., Guerrero-Medina, P.J., 2015. Storage effect on phenols and on the antioxidant activity of extracts from *Anemopsis californica* and inhibition of elastase enzyme. J. Chem., http://dx.doi.org/10.1155/2015/602136.

Elliott, G.N., Worgan, H., Broadhurst, D., Draper, J., Scullion, J., 2007. Soil differentiation using fingerprint Fourier transform infrared spectroscopy, chemometrics and genetic algorithm-based feature selection. Soil Biol. Biochem. 39, 2888–2896.

EMEA, 2001. European Agency for the Evaluation of Medicinal Products, Final Proposals for Revision of the Notes for Guidance on Quality of Herbal Medicinal Products, The European Agency for the Evaluation of Medicinal Products. EMEA, London, pp. 1–8.

Fang, Z., Bhandari, B., 2010. Encapsulation of polyphenols – a review. Trends Food Sci. Technol. 21, 510–523.

Friedman, M., Jürgens, H.S., 2000. Effect of pH on the stability of plant phenolic compounds. J. Agric. Food Chem. 48, 2101–2110.

Goyal, P., Goyal, K., Kumar, S.G.V., Singh, A.O.M.P.K., Mishra, D.N., 2005. Liposomal drug delivery systems – clinical applications. Acta Pharm. 55, 1–25.

Greenspan, L., 1977. Humidity fixed points of binary saturated aqueous solutions. J. Res. Natl. Bur. Stand 81, 89–96.

Hossain, M.A., Mizanur Rahman, S.M., 2015. Isolation and characterisation of flavonoids from the leaves of medicinal plant Orthosiphon stamineus. Arab. J. Chem. 8, 218–221.

Hussain, K., Majeed, M.T., Ismail, Z., Sadikun, A., Ibrahim, P., 2009. Traditional and complementary medicines: quality assessment strategies and safe usage. Southern Med. Rev. 2, 19–23.

ICH, 1996. Q2B Validation of Analytical Procedures: Methodology. Department of Health and Human Services Food and Drug Administration, U.S.

ICH, 2003. Stability Testing Guidelines: Stability Testing of New Drug Substances and Products. International Conference on Harmonisation , pp. 1–16.
Khalid, H., Zhari, I., Amirin, S., Pazilah, I., 2011. Accelerated stability and chemical kinetics of ethanol extracts of fruit of *Piper sarmentosum* using high performance liquid chromatography. Iran J. Pharm. Res. 10, 403–413.
Kotsiou, K., Tasioula-Margari, M., 2016. Monitoring the phenolic compounds of Greek extra-virgin olive oils during storage. Food Chem. 200, 255–262.
Li, S., Han, Q., Qiao, C., Song, J., Lung Cheng, C., Xu, H., 2008. Chemical markers for the quality control of herbal medicines: an overview. Chin. Med. 3, 1–16.
Marsh, K.N., 1987. Recommended Reference Materials for the Realization of Physicochemical Properties. Blackwell Scientific Publication, Oxford.
Munin, A., Edwards-Lévy, F., 2011. Encapsulation of natural polyphenolic compounds; a review. Pharmaceutics 3, 793–829.
Murphy, B., Murphy, C., Hathaway, B.J.A., 1997. Working Method Approach for Introductory Physical Chemistry Calculations. Royal Society of Chemistry, Cambridge.
Pourrat, H., Barthomeuf, C., Pourrat, A., Cottier, P.-E., Ibrahim, H., 1995. Stabilization of Octastatin, a somatostatin analogue, Preparation of freeze-dried products for parenteral injection. Biol. Pharm. Bull. 18, 766–771.
Pugh, J., 2002. Kinetics and Product Stability, Textbook of Pharmaceutics the Science of Dosage Form Design, 2nd ed. Churchill Livingstone, London, pp. 101–112.
Rawlins, E., 1977. Bentley's Textbook of Pharmaceutics. Bailliere Tindall, London.
Rice-Evans, C.A., Miller, N.J., Paganga, G., 1996. Structure–antioxidant activity relationships of flavonoids and phenolic acids. Free Radic. Biol. Med. 20, 933–956.
Sahib, H.B., Aisha, A.F., Yam, M.F., Asmawi, M.Z., Ismail, Z., Salhimi, S.M., Othman, N.H., Abdul Majid, A.M.S., 2009. Anti-angiogenic and antioxidant properties of *Orthosiphon stamineus* Benth. methanolic leaves extract. Int. J. Pharmacol. 5, 162–167.
Siddiqui, M.J.A., Ismail, Z., 2011. Simultaneous analysis of bioactive markers from *Orthosiphon stamineus* Benth leaves extracts by reverse phase high performance liquid chromatography. Trop. J. Pharm. Res. 10, 97–103.
Tezuka, Y., Stampoulis, P., Banskota, A.H., Awale, S., Tran, K.Q., Saiki, I., Kadota, S., 2000. Constituents of the Vietnamese medicinal plant *Orthosiphon stamineus*. Chem. Pharm. Bull. 48, 1711–1719.
Volf, I., Ignat, I., Neamtu, M., Popa, V.I., 2014. Thermal stability, antioxidant activity, and photo-oxidation of natural polyphenols. Chem. Pap. 68, 121–129.
Waterman, K.C., Adami, R.C., Alsante, K.M., Antipas, A.S., Arenson, D.R., Carrier, R., Hong, J., Landis, M.S., Lombardo, F., Shah, J.C., Shalaev, E., Smith, S.W., Wang, H., 2002. Hydrolysis in pharmaceutical formulations. Pharm. Dev. Technol. 7, 113–146.
WHO, 1996. WHO Expert Committee on Specifications for Pharmaceutical Preparations, Guidelines for the Assessment of Herbal Medicines. WHO, Geneva.
Yam, M.F., Asmawi, M.Z., Basir, R., 2008. An investigation of the anti-inflammatory and analgesic effects of *Orthosiphon stamineus* leaf extract. J. Med. Food 11, 362–368.
Young, J.F., 1967. Humidity control in the laboratory using salt solutions – a review. J. Appl. Chem. 17, 241–245.
Zavoi, S., Fetea, F., Ranga, F., Raluca, M.P., Baciu, A., Socaciu, C., 2011. Comparative fingerprint and extraction yield of medicinal herb phenolics with hepatoprotective potential, as determined by UV-Vis and FT-MIR spectroscopy. Not. Bot. Horti. Agrobot. Cluj. Napoca 39, 82–89.